Partial Discharge Inception and Propagation Characteristics of Magnet Wire for Inverter-fed Motor under Surge Voltage Application

Naoki Hayakawa, Masato Morikawa
Department of Electrical Engineering and Computer Science
Nagoya University
Furo-cho, Chikusa-ku, Nagoya, 464-8603, Japan

and **Hitoshi Okubo**
EcoTopia Science Institute
Nagoya University
Furo-cho, Chikusa-ku, Nagoya, 464-8603, Japan

ABSTRACT

In inverter-fed motor coils, surge voltages with the rise time of several tens or hundreds of nano-second may cause partial discharge (PD) and degradation of electrical insulation performance of the inverter-fed motor coils. This paper discusses PD inception characteristics as well as PD propagation characteristics after PD inception for magnet wire of inverter-fed motor under surge voltage application. Experimental results firstly revealed that PD inception voltage (PDIV) decreased with the increase in the length of enamel-coated wire, which was evaluated in terms of the stressed wire contact length under surge voltage application, i.e. size effect. We proposed a regression line for the size effect on PDIV for the electrical insulation design of inverter-fed motor coils. Secondly, PD propagation characteristics were also investigated under the higher voltage application, and their mechanisms were discussed in terms of generation probability of initial electrons, space charge behavior in the wedge-shaped air gap, charging on the enamel surface and so on.

Index Terms — Inverter-fed motor, inverter surge, partial discharge, inception voltage, initial electron, charge behavior.

1 INTRODUCTION

THE operating voltage of inverter-fed motors is being increased for higher performance, e.g., higher power output and compactness. Inverter-fed motors utilize power electronic devices such as IGBTs with high-speed switching ability, and they are exposed to transient surge voltage, so called inverter surge. Inverter surge with the rise time of several tens or hundreds of nano-second in inverter-fed motor coils may cause partial discharge (PD) and degradation of electrical insulation performance. Therefore, rational electrical insulation design and evaluation techniques for the inverter-fed motors are strongly required, which should take account of the PD mechanisms under surge voltage application [1-4].

From the above background, we have been investigating the PD inception characteristics as well as PD propagation characteristics after PD inception for inverter-fed motor coil samples under surge voltage application [5-7]. In this paper, we focused on the PD inception voltages (PDIV) of inverter-fed motor coil samples with different lengths of enamel-coated wire under surge and ac voltage application. Together with the dependence of PDIV on the repetition rate and polarity reversal of the applied surge voltage, PD inception mechanisms under surge voltage application were discussed and compared with those under ac voltage application. Moreover, focusing on the PD propagation after PD inception, we measured the transition of number of PD generation, PD light pulses and PD light emission images under different surge voltages higher than PDIV. These PD propagation characteristics were discussed from the viewpoint of charge behavior in the wedge-shaped air gap and on the enamel surface.

Manuscript received on 20 February 2006, in final form 26 July 2006.

1070-9878/07/$25.00 © 2007 IEEE

2 EXPERIMENTAL SETUP AND PROCEDURE

2.1 EXPERIMENTAL SETUP FOR PD INCEPTION CHARACTERISTICS

Figure 1 shows test samples used in this experiment: (a) twisted pair samples and (b) coil samples. Each sample was composed of two enamel-coated copper wires. The conductor diameter is 0.845 mm, the coated thickness is 0.03 mm (polyester imide: 0.023 mm, polyamide imide: 0.007 mm) and the dielectric constant is 3.85. The twisted pitch and length of the twisted pair samples are 7 mm and 130 mm, respectively. On the other hand, the coil samples were used as an intermediate model between the simplified twisted pair and the actual motor winding such as a random wound motor. In the coil samples, two enamel-coated copper wires were wound in parallel on 1 layer around a PMMA cylinder with the diameter of 50 mm. The turn numbers of the coil samples are 1, 5, 10, 20, 40, 100 and 200, respectively. Figure 2 shows the relationship between the turn number and the wire contact length of the coil samples. The wire contact length of the coil samples is confirmed to be proportional to the turn number. The capacitance of the coil samples is also proportional to the wire contact length, i.e. turn number.

The experimental setup for the measurement of PD characteristics of the test samples is shown in Figure 3. For both twisted pair and coil samples, after surface cleaning by alcohol, one of the copper wires was grounded, and surge or

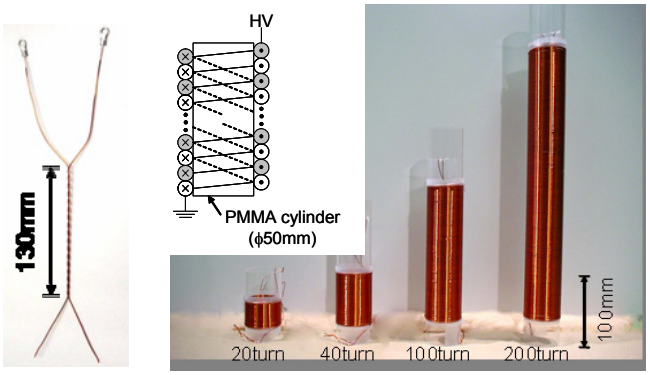

(a) Twisted pair (b) Coil samples

Figure 1. Test samples.

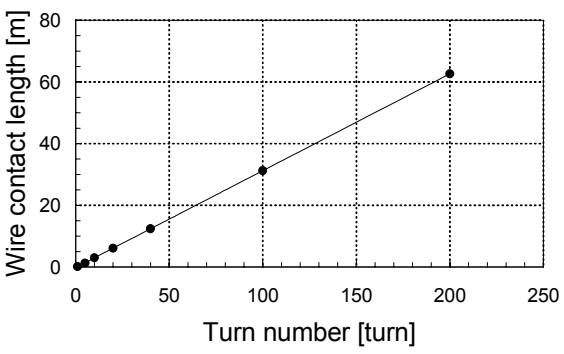

Figure 2. Relationship between turn number and wire contact length of coil samples.

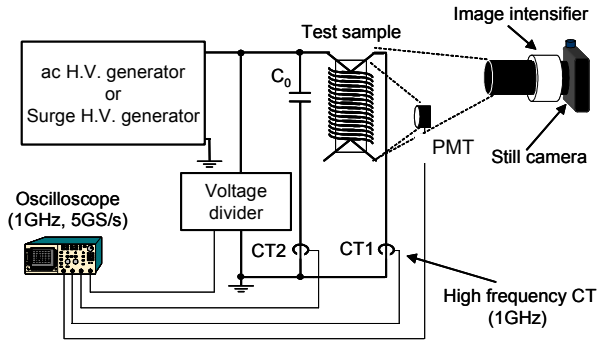

Figure 3. Experimental setup for PD inception characteristics.

ac high voltage was applied to the other wire. A complementary capacitor with capacitance C_0 was connected in parallel with the test samples. By arranging the value of C_0 for each test sample, the total capacitance C_{Total} of the test sample and the complementary capacitor was set at around 6,000 pF or 10,000 pF, which enabled us to control the rise time t_r of the applied surge voltage within 450 ns to 600 ns (average t_r=520 ns) for C_{Total}=6,000 pF or within 700 ns to 900 ns (average t_r=830 ns) for C_{Total}=10,000 pF. The repetition rate of the surge voltage f was within 6 pps (pulse per second) to 60 pps. Single shot, positive or negative shot of the surge voltage were also possible. The time width of the single shot was 1 μs. The frequency of ac voltage was 60 Hz.

PD measurement with current pulse detection by CT under surge voltage is generally difficult because of a large charging current due to steep wavefront of the applied surge voltage. Thus, optical PD measurement by photo multiplier tube (PMT) is often used under surge voltage application. Thus, in this paper, PDIV of the test samples was measured by PMT under both surge and ac voltage applications. PD light emission images were also taken by a still camera through an image intensifier (I.I.) with setting the exposure time to 5 s. We also measured the PD current pulse signal under ac voltage application through high frequency CT (1 GHz); CT1 for the test sample and CT2 for the complementary capacitor. According to our previous research using twisted pair [5], PDIV measured by PMT was at most 5 % higher than that by CT with the PD detection sensitivity of about 1 pC, which may be attributed to the invisible PD in the blind region of test sample. Environmental conditions such as temperature, pressure and humidity were controlled in the shielding room with air conditioning.

2.2 EXPERIMENTAL SETUP FOR TRANSITION OF PD CHARACTERISTICS

Figure 4 shows the experimental setup for the measurement of PD propagation characteristics of a twisted pair sample with the same specification as those in 2.1. On the other hand, the inverter surge generation circuit is different from that in 2.1, which consists of dc high voltage supply, high voltage semiconductor switch, pulse generator and coaxial cable. It can generate damped oscillating surge voltages with flexible surge parameters such as peak value, rise time, pulse width,

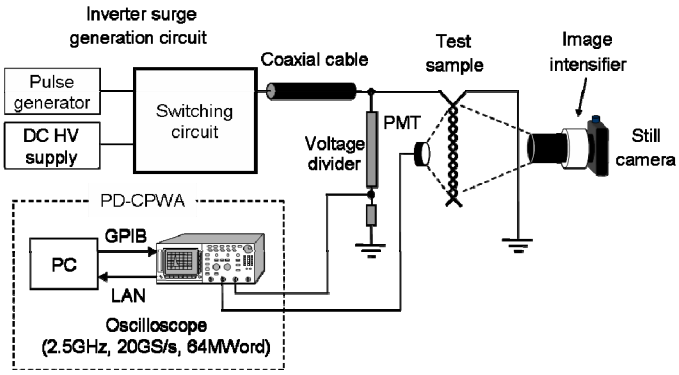

Figure 4. Experimental setup and measurement system for transition of PD characteristics.

repetition rate and polarity. In this experiment, the peak value V_a was 0 ~ 1710 V_{peak}, t_r=120 ns, the pulse width was 10 μs and f=1000 pps, respectively.

PDIV was measured by PMT, and a still camera through an I.I. also took PD light emission images. The detected PD light intensity signals were recorded by an oscilloscope (2.5 GHz, 20 GS/s, 64 MWord) and analyzed by the partial discharge current pulse waveform analysis (PD-CPWA) method [8]. PD-CPWA is a PD detection/analysis system developed for the purpose of pursuing the transition of PD current pulse waveforms, and it was applied to PD light intensity waveforms by PMT in this experiment. PDIV was defined as the peak value of the applied voltage, and converted into the value at the standard atmospheric condition (20 ˚C, 0.1 MPa).

3 PD INCEPTION CHARACTERISTICS

3.1 PD GENERATION CHARACTERISTICS

Typical PD light intensity and applied voltage waveforms at PD inception are shown in Figure 5 under (a) surge voltage application (t_r=520 ns, f=60 pps, positive polarity) and (b) ac voltage application (60 Hz), respectively, for the 100 turn coil sample. The surge PDIV was 1078 V_{peak} and the ac PDIV was 716 V_{peak}, respectively. In both figures, PD signal was detected at around the peak of the applied voltage waveform.

Figure 6 shows (a) a picture of 20 turn coil sample and (b) PD light emission image at V_a=1400 V_{peak} under surge voltage application (t_r=520 ns, f=60 pps, positive polarity). Using mirrors at left and right back of the coil sample, as shown in Figure 6a, PD light emission image at any location of the sample could be observed. PD light emission image was so faint at around PDIV (=1276 V_{peak}). With the increase in V_a, the PD light emission image became clear and was found to be spread over the whole surface of the coil sample in Figure 6b. Thus, PD phenomena of inverter-fed motor coil samples under surge voltage application could be verified, located and visualized as a light emission image by the optical PD measurement technique.

3.2 SIZE EFFECT ON PD INCEPTION VOLTAGE

PDIV of twisted pair and coil samples under surge voltage application (f=60 pps, positive and negative polarity) are shown in Figure 7, where the history of PDIV for sequential

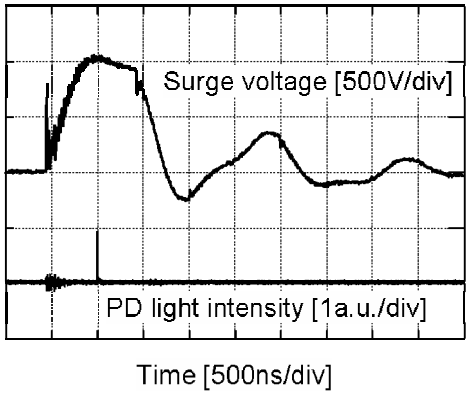

(a) Surge voltage (t_r=520 ns, f=60 pps, positive polarity)

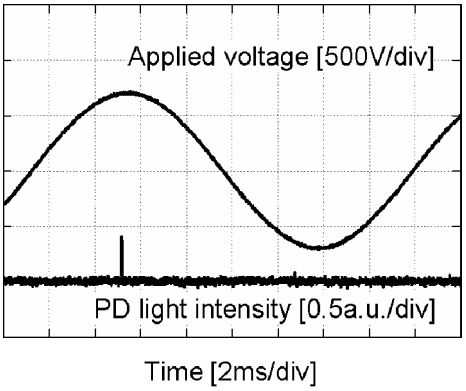

(b) ac voltage (60Hz)

Figure 5. Applied surge voltage and PD light intensity waveforms (100 turn coil sample).

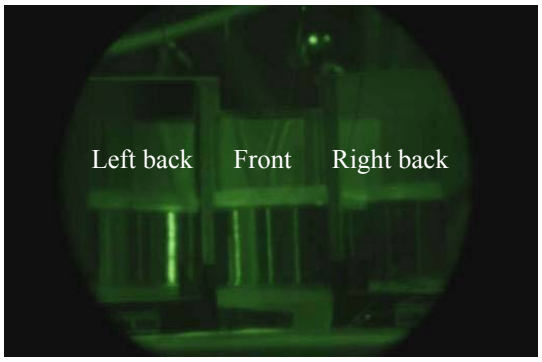

(a) Picture of 20 turn coil sample

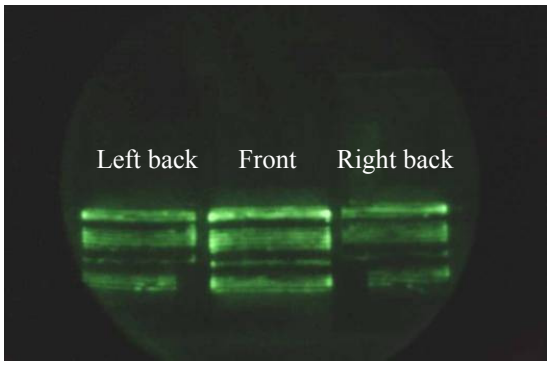

(b) PD light emission image at V_a=1400V_{peak}

Figure 6. Surge PD light emission images (20 turn coil sample, t_r=520 ns, f=60 pps, positive polarity).

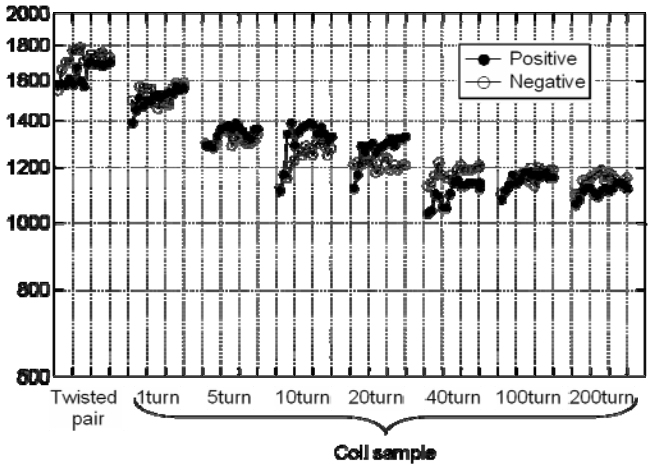

Figure 7. Surge PDIV for different test samples (t_r=520 ns, f=60 pps).

shots of measurements is designated for each sample. PDIV decreased with the increase in the turn number of the coil samples, i.e. wire contact length. There existed a small conditioning effect and no polarity effect in PDIV. Then, the last 5 PDIVs which seem to be stable in 15 measurements will be taken for the evaluation and analysis of PDIV, hereinafter.

Figure 8 shows surge PDIV for (a) t_r=520 ns, (b) t_r=830 ns and ac PDIV as a function of wire contact length. Each figure represents the average value and the standard deviation of PDIV under different voltage applications. In the case of repetitive positive-negative surge voltage application, the time interval of surge application was 5 s. In each case, PDIV decreased with the increase in the wire contact length. For example, PDIV of 100 turn coil decreased into 85 % of PDIV of 1 turn coil under surge (positive, single) voltage application. Such a decrease in PDIV with the increase in the stressed length, area or volume is generally referred to as the "size effect". The PD threshold behavior on the size effect is attributed to the increase in the initial electrons in the wedge-shaped air gap between enamel-coated copper conductors as well as on the enamel surface. With the increase in the turn number of coil samples, i.e. stressed wire contact length, the generation probability of initial electrons would be increased, and then PDIV could be decreased.

In order to quantitatively evaluate the size effect, the regression lines in Figure 8 for the coil samples were expressed by the following equation (1):

$$\mathrm{PDIV} = \mathrm{A} \times \lambda^{-\frac{1}{\mathrm{B}}} \quad (1)$$

where A and B are constants, and λ is the wire contact length. Table 1 summarizes the values of A and B under different voltage conditions. PDIV decreased with the increase in λ, repetition rate of surge voltage application and polarity reversal. The surge PDIV (f=60 pps) normalized by ac PDIV (60 Hz), referred to as the impulse ratio, was 1.4 to 2.0. The impulse ratio for t_r=830 ns tended to decrease with the increase in λ; which means that the generation probability of initial electrons would increase under the longer contact length of stressed wire or the larger volume of wedge-shaped air gap between the enamel-coated copper conductors.

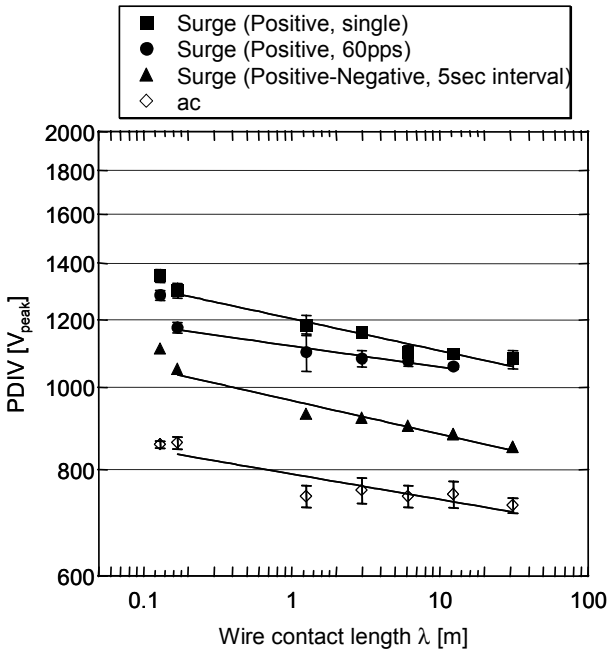

(a) t_r=520 ns (C_{Total}=6,000 pF)

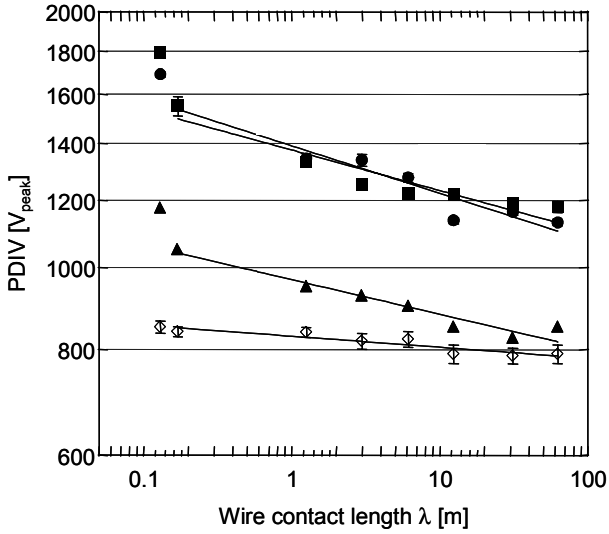

(b) t_r=830 ns (C_{Total}=10,000 pF)

Figure 8. PDIV as a function of wire contact length λ.

Table 1. Constant A and B under different voltage applications.

C_{total}	t_r=520ns		t_r=830ns	
	A	B	A	B
Surge (Positive, single)	1205	26.5	1375	21.0
Surge (Positive, 60pps)	1118	40.5	1392	17.8
Surge (Positive-Negative)	965	25.4	967	24.5
ac	790	33.3	829	77.9

In addition, PDIV for t_r=520 ns was lower than that for t_r=830 ns. Thus, PDIV would be influenced not only by the rise time of the applied surge voltage, but also by the other factors on surge voltage waveform. Furthermore, the surge PDIV at the polarity reversal was lower than those for single

shot or repetitive shot with an identical polarity. This may suggest the possibility of charge generation at the applied surge voltage lower than PDIV.

4 PD PROPAGATION CHARACTERISTICS

4.1 TRANSITION OF PD CHARACTERISTICS

In this section, PD propagation characteristics after PD inception are discussed using a twisted pair sample. Figure 9 shows typical applied surge voltage and PD light intensity waveforms at V_a=1500 V_{peak} under repetitive surge voltage application (t_r=120 ns, f=1000 pps). PDs were usually generated at both the instant of rise and fall time regions of surge voltage waveform. The PDIV was obtained as 1170 V_{peak} for the twisted pair sample used in this experiment.

Figure 10 shows the transition of peak value of PD light intensity for different applied voltages higher than PDIV (positive polarity, f=1000 pps) for the twisted pair sample with PDIV=1170 V_{peak}. PD generation was intermittent in Figures 10a (V_a=1170 V_{peak}=PDIV) and 10b (V_a=1300 V_{peak}=1.11 × PDIV) and became continuous with the larger intensity in Figure 10c (V_a=1710 V_{peak}=1.46 × PDIV) with the higher V_a. The number of PD generation in Figure 10c reached 2000/s, which means that PD was generated 2 times in each voltage application of f=1000 pps, as was shown in

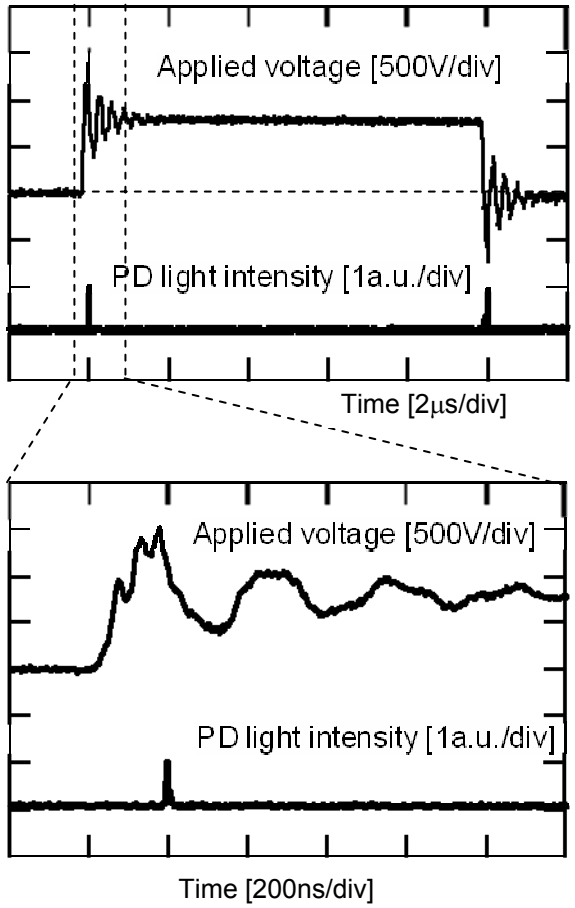

Figure 9. Applied surge voltage and PD light intensity waveforms for the twisted pair sample (t_r=120 ns, f=1000 pps).

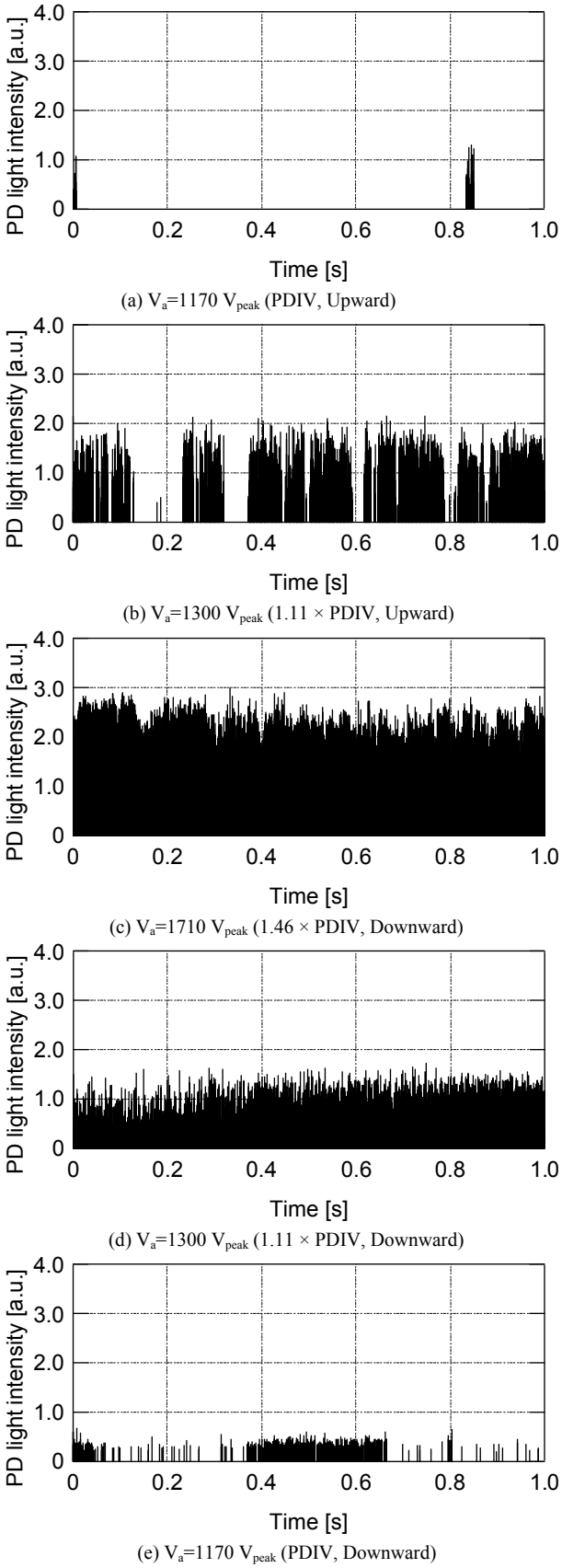

Figure 10. Transition of PD light intensity as a function of voltage enhancement and reduction (Twisted pair sample, t_r=120 ns, f=1000 pps).

Figure 9. In the downward process of V_a in Figure 10d (V_a=1300 V_{peak}=1.11 × PDIV), PD generation was still continuous with 2000 pps, in spite of the same V_a as in Figure 10b, and became intermittent with the smaller intensity in Figure 10e (V_a=1170 V_{peak}=PDIV). PD extinction voltage (PDEV) was 1080 V_{peak} lower than PDIV (1170 V_{peak}).

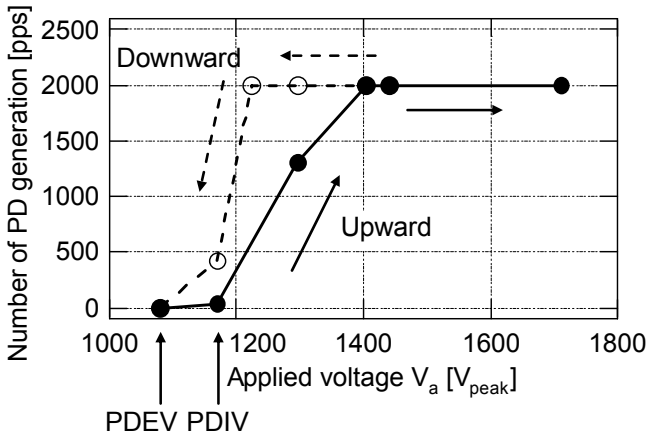

Figure 11. Transition of number of PD generation as a function of applied voltage (Twisted pair sample, t_r=120 ns, f=1000 pps)

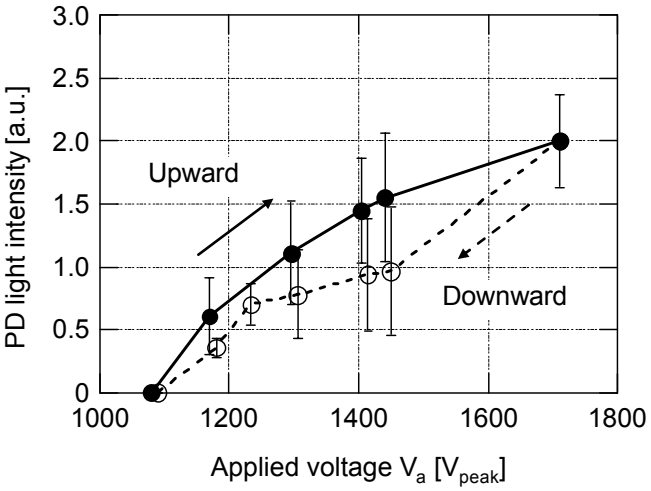

Figure 12. Transition of PD light intensity as a function of applied voltage (Twisted pair sample, t_r=120 ns, f=1000 pps)

Figure 11 and 12 summarize the transition of the number of PD generation and PD light intensity, respectively, as a function of applied voltage. The number of PD generation in Figure 11 clearly shows the hysteresis characteristics. PD light intensity in Figure 12 also shows the hysteresis characteristics, where the intensity in the downward process was smaller than that in the upward process. These results mean that in the downward process of V_a, smaller PD was frequently generated compared with that in the upward process. Figure 13 shows the PD light emission images at (b) V_a=1300 V_{peak} (1.11 × PDIV, upward), (c) V_a=1710 V_{peak} (1.46 × PDIV, upward), (d) V_a=1300 V_{peak} (1.11 × PDIV, downward) and (e) V_a=1170 V_{peak} (PDIV, downward). PD light emission at the both ends of the sample was stronger in the upward process (Figures 13b and 13c), whereas that in the middle area remained in the downward process (Figure 13e).

4.2 DISCUSSION OF PD GENERATION MECHANISMS

From the above experimental results, PD generation mechanisms were discussed. PD characteristics can be classified into the following three regions:

(1) V_a=PDIV
(2) PDIV < V_a < 1.1×PDIV
(3) V_a >1.1×PDIV

Here, 1.1×PDIV corresponds to the applied voltage, where the number of PD generation starts to increase distinctively, as shown in Figure 11.

In the region (1), the generation probability of initial electrons would be low, because the time exposed to high electric field stress for the small wedge-shaped air gap was short under the damped oscillating surge voltage. For this reason, PD generation was unstable, as shown in Figure 10a.

In the region (2), positive ions, negative ions and electrons would already exist by repetitive PDs at the higher applied voltage. Therefore, the number of PD generation would increase gradually by the initial electrons originated from negative ions and electrons. However, PD generation was still intermittent, as shown in Figure 10b, because the time

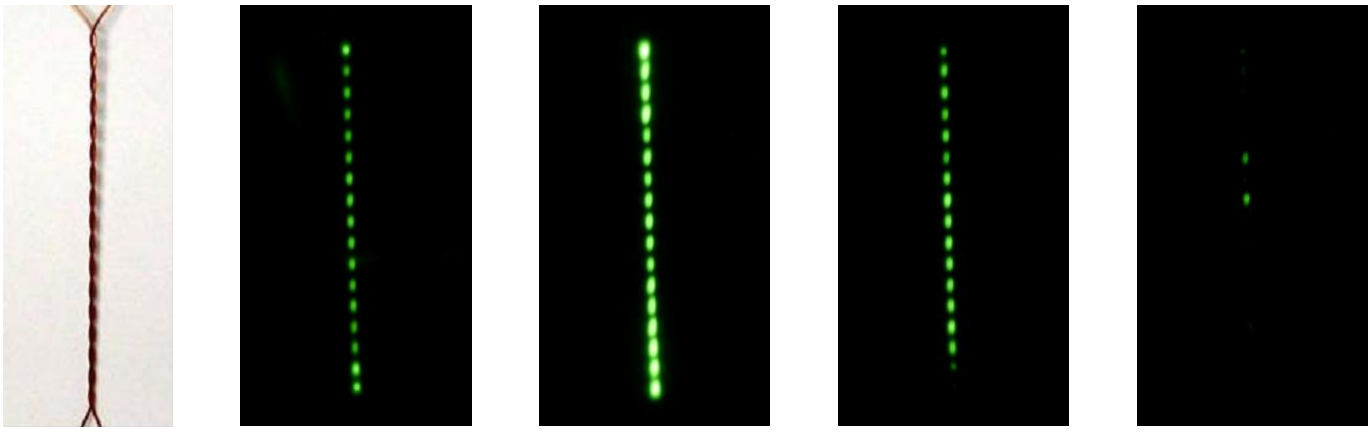

(a) Twisted pair sample | (b) V_a=1300 V_{peak} (1.11 × PDIV, Upward) | (c) V_a=1710 V_{peak} (1.46 × PDIV, Upward) | (d) V_a=1300V_{peak} (1.11 × PDIV, Downward) | (e) V_a=1170V_{peak} (PDIV, Downward)

Figure 13. Transition of PD light emission images (Twisted pair sample, t_r=120 ns, f=1000 pps).

exposed to high electric field stress for the wedge-shaped air gap was still as short as several hundreds of nano-second under the damped oscillating surge voltage.

On the other hand, in the region (3), the generation probability of initial electrons for several hundreds of nano-second would increase sufficiently, because the electric field stress in the wedge-shaped air gap is high enough in such a high voltage region. The charge density and distribution in the wedge-shaped air gap and on the enamel surface can also affect the successive PD generation and its magnitude, which would bring about the hysteresis characteristics and the scattering of PD light intensity, as shown in Figures 10 to 12. PD could be generated at both the instant of rise and fall time regions of surge voltage waveform because of the charge behavior in the wedge-shaped air gap, and then the number of PD generation reached 2000 pps.

5 CONCLUSIONS

PD inception characteristics and PD propagation characteristics after PD inception for twisted pair and coil samples under surge voltage application were obtained and quantitatively evaluated. The main results are summarized as follows:

(1) PDIV decreased with the increase in the wire length, which was evaluated in terms of the stressed wire contact length, i.e. size effect.
(2) The regression lines for the size effect on PDIV were quantitatively evaluated and expressed in the form of $PDIV=A \times \lambda^{-1/B}$, where A and B are constants and λ is the wire contact length.
(3) PDs under repetitive surge voltage application were usually generated at both the instant of rise and fall time regions of surge voltage waveform.
(4) Number of PD generation increased with the increase in the applied voltage under repetitive surge voltage application. Number of PD generation and PD light intensity exhibited hysteresis characteristics.
(5) PD generation mechanisms were discussed from the viewpoint of the charge behavior in the wedge-shaped air gap and on the enamel surface.

REFERENCES

[1] M. Kaufhold, "Stress Related Challenges of Converter Fed Drives Survey of Requirements, Concepts and Strategies", INSUCON, pp. 131-136, 2002.
[2] S. Grzybowski and N. P. Kota, "Lifetime Characteristics of Magnet Wires under Multistress Conditions", IEEE CEIDP, pp. 605-608, 2005.
[3] K. Bauer, M. Kaufhold, A. Maeurer and K. Schaefer, "Machine Insulation for Converter Fed Low Voltage Drive Systems-Requirements and Design", INSUCON, pp. 362-366, 2002.
[4] D. Fabiani, G. C. Montanari, A. Cavallini and G. Mazzanti, "Relation Between Space Charge Accumulation and Partial Discharge Activity in Enameled Wires Under PWM-like Voltage Waveforms", IEEE Trans. Dielectr. Electr. Insul., Vol. 11, pp. 393-405, 2004.
[5] N. Hayakawa and H. Okubo, "Partial Discharge Characteristics of Inverter-Fed Motor Coil Samples under AC and Surge Voltage Conditions", IEEE Elect. Insul. Mag., Vol. 21, No. 1, pp. 5-10, 2005.
[6] M. Morikawa, N. Hayakawa and H. Okubo, "Partial Discharge Inception and Degradation Characteristics of Inverter-Fed Motor Sample under Surge Voltage Condition", IEEE CEIDP, pp. 426-429, 2005.
[7] H. Okubo, Y. Lu, M. Morikawa and N. Hayakawa, "Partial Discharge Inception Characteristics Influenced by Stressed Wire Length of Inverter-Fed Motor", IEEE CEIDP, pp. 442-445, 2004.
[8] H. Okubo, N. Hayakawa, "A Novel Technique for Partial Discharge and Breakdown Investigation Based on Current Pulse Waveform Analysis", IEEE Trans. Dielectr. Electr. Insul., Vol. 12, pp. 736-744, 2005.

Naoki Hayakawa (M'90) was born on 9 September 1962. He received the Ph.D. degree in 1991 in electrical engineering from Nagoya University. Since 1990, he has been at Nagoya University and presently he is an Associate Professor of Nagoya University at the Department of Electrical Engineering and Computer Science. From 2001 to 2002, he was a guest scientist at the Forschungszentrum Karlsruhe /Germany. He is a member of IEEE and IEE of Japan.

Masato Morikawa was born on 17 March 1982. He received the B.S. degree in 2004 in electrical engineering from Nagoya University. Currently, he is a Master Course student at Nagoya University in the Department of Electrical Engineering and Computer Science.

Hitoshi Okubo (M'81) was born on 29 October 1948. He received the Ph.D. degree in 1984 in electrical engineering from Nagoya University. He joined Toshiba Corporation, Japan in 1973 and was a Manager of HV laboratory of Toshiba. From 1976 to 1978, he was at the RWTH Aachen, Germany and the TU Munich, Germany. In 1989 he was an Associate Professor and presently he is a Professor at Nagoya University in the EcoTopia Science Institute. He is a member of IEEE, IEE of Japan, VDE and CIGRE.